Cell

Molecular Architecture of Annelid Nerve Cord Supports Common Origin of Nervous System Centralization in Bilateria

Alexandru S. Denes,[1,6] Gáspár Jékely,[1,6] Patrick R.H. Steinmetz,[1,4] Florian Raible,[1] Heidi Snyman,[1] Benjamin Prud'homme,[2,5] David E.K. Ferrier,[3] Guillaume Balavoine,[2] and Detlev Arendt[1,*]
[1] Developmental Biology Unit, European Molecular Biology Laboratory, Heidelberg, 69117, Germany
[2] Centre de Génétique Moléculaire, CNRS, Gif-sur-Yvette 91198, France
[3] Department of Zoology, University of Oxford, Oxford, OX1 3PS, United Kingdom
[4] Present address: Sars Centre, Thormøhlensgt. 55, N-5008 Bergen, Norway.
[5] Present address: Institut de Biologie du Developpement de Marseille Luminy, UMR 6216 Case 907, Parc Scientifique de Luminy, 13288 Marseille Cedex 09, France.
[6] These authors contributed equally to this work.
*Correspondence: arendt@embl.de
DOI 10.1016/j.cell.2007.02.040

SUMMARY

To elucidate the evolutionary origin of nervous system centralization, we investigated the molecular architecture of the trunk nervous system in the annelid *Platynereis dumerilii.* Annelids belong to Bilateria, an evolutionary lineage of bilateral animals that also includes vertebrates and insects. Comparing nervous system development in annelids to that of other bilaterians could provide valuable information about the common ancestor of all Bilateria. We find that the *Platynereis* neuroectoderm is subdivided into longitudinal progenitor domains by partially overlapping expression regions of *nk* and *pax* genes. These domains match corresponding domains in the vertebrate neural tube and give rise to conserved neural cell types. As in vertebrates, neural patterning genes are sensitive to Bmp signaling. Our data indicate that this mediolateral architecture was present in the last common bilaterian ancestor and thus support a common origin of nervous system centralization in Bilateria.

INTRODUCTION

In 1875 Anton Dohrn proposed that vertebrates inherited their central nervous systems (CNSs) from an annelid-like ancestor and that vertebrates inverted their dorsoventral body axis during their evolution ("annelid theory"; Dohrn, 1875). This view was in conflict with the notion that the invertebrate and vertebrate CNS evolved on opposite body sides ("Gastroneuralia-Notoneuralia concept"; Hatschek, 1878). More than a decade ago the comparative molecular analysis of the conserved Bmp (Dpp) dorsoventral patterning cascades revived the idea of dorsoventral axis inversion (reviewed in Arendt and Nübler-Jung, 1994; De Robertis and Sasai, 1996), and reinitiated a discussion on the possible homology of the ventral invertebrate and dorsal vertebrate CNS. This was fuelled by molecular data revealing a similar mediolateral sequence of *nk2.2*+, *gsx*+, and *msx*+ neurogenic domains in the insect and vertebrate neuroectoderm (Arendt and Nübler-Jung, 1999). *Nk6* orthologs also appear to play a conserved role in neuroectodermal mediolateral patterning because their initial neuroectodermal expression in *Drosophila* is medially restricted, as it is in vertebrates (Cheesman et al., 2004). More recently it was found that the expression of neural patterning genes is sensitive to threshold-dependent Bmp-mediated repression in both groups (Mizutani et al., 2006).

The overall similarity in mediolateral patterning between vertebrate and fly is limited, however. While in *Drosophila* the *nk2.2* (*vnd*) and *gsx* (*ind*) neurogenic domains are directly abutting (Weiss et al., 1998), there is a large gap between the *nk2.2* and *gsx* (*gsh1, gsh2*) progenitor domains in the vertebrate neural tube that is filled by a broad region of *pax6* and *dbx* expression (Briscoe et al., 2000; Kriks et al., 2005), while the *Drosophila pax6* orthologs do not play an early role in neuroectoderm regionalization (Kammermeier et al., 2001). Patterns of other conserved regionalization genes are also different between vertebrate and fly. For example, *pax3/7* orthologs are active in transverse stripes in *Drosophila* but are active in lateral longitudinal domains in the vertebrate neural tube (Arendt and Nübler-Jung, 1999). Fly and vertebrate also differ in their mediolateral distribution of neuron types. For example, somatic motoneurons emerge from only the *pax6+/nk6+* progenitor domain in vertebrates (Jessell, 2000) but from all mediolateral levels in *Drosophila* (Bossing et al., 1996; Schmidt et al., 1997).

At odds with the notion of evolutionary conservation of the CNS in Bilateria, recent large-scale expression analyses of neural genes in the hemichordate enteropneust *Saccoglossus* (a distant deuterostome relative of the vertebrates) revealed expression of mediolateral patterning genes such as *pax6, dbx,* and *msx* and of neural differentiation markers around the circumference of the embryo (Lowe et al., 2003, 2006) Also, Bmp signaling does not repress neural gene expression in the enteropneust (Lowe et al., 2006). This reinforced the view that centralization of the nervous system was acquired independently in the deuterostome and protostome lines of evolution (Holland, 2003; Lowe et al., 2003, 2006).

To broaden the phylogenetic perspective on CNS evolution, we decided to look into the third large superphylum of bilaterian animals, the Lophotrochozoa (Halanych et al., 1995). We chose to investigate the mediolateral molecular architecture of the developing trunk CNS in the polychaete annelid *Platynereis dumerilii*. We report that from medial to lateral the *Platynereis* ventral trunk neuroectoderm is subdivided into adjacent *nk2.2+/nk6+*, *pax6+/nk6+*, *pax6+/pax3/7+*, and *msx+/pax3/7+* longitudinal progenitor domains in striking correspondence to the mediolateral subdivision of the vertebrate neural tube. Beyond that, similar neuron types emerge from corresponding domains in *Platynereis* and vertebrate, such as serotonergic neurons modulating locomotor activity and cholinergic somatic motoneurons. Finally, we report that *bmp2/4* is expressed on the dorsal body side in *Platynereis* and that Bmp4 regulates mediolateral patterning genes in the *Platynereis* neuroectoderm. This overall similarity surpasses that documented previously for vertebrate and fly and indicates that a CNS already existed in Urbilateria.

RESULTS

Formation of a Ventral Neuroectoderm and Neurogenesis in the *Platynereis* Trunk Nervous System

As a prerequisite for our study, we first explored how the *Platynereis* trunk neuroectoderm initially forms, where and when neurogenesis is initiated, and how it progresses in the *Platynereis* neuroepithelium. During gastrulation, the edges of the proliferating trunk ectoderm (arrows in Figure 1A) meet and fuse at the ventral midline at around 24 hpf (Anderson, 1966; Wilson, 1892). Using in vivo time-lapse imaging, we tracked individual cells and showed that the fusion progresses from posterior to anterior in a zipper-like manner (Figures 1B–1D; Movie S1). During this process, the future midline takes the shape of a "Y" (orange in Figures 1B and 1E). While the more anterior cells (representing the two arms of the Y) are still located on the two sides of the future mouth (stomodeum), the more posterior cells have met already. Fusion is complete at 48 hpf.

Using the neural differentiation markers *elav* and *synaptotagmin*, we determined the timing and spatial extent of early neurogenesis and, thus, the extent of the *Platynereis* neuroectoderm. Elav is an RNA-binding protein specific for postmitotic differentiating neurons (Soller and White, 2004). Synaptotagmin is a transmembrane protein required for synaptic vesicle trafficking (Poskanzer et al., 2003). To investigate gene expression at the cellular level with the resolution provided by confocal microscopy we combined whole-mount in situ hybridization (WMISH) with whole-mount reflection confocal laser scanning microscopy, a newly developed technique that visualizes NBT/BCIP staining by reflection of the confocal laser beam (Jékely and Arendt, 2007). In the course of neuronal differentiation, *Platynereis synaptotagmin* is turned on 8 to 10 hr after *elav*. The first differentiating neurons are present at early larval stages (Figures 1E, 1G, and 1H). Larger patches of differentiating neurons appear at 38 hpf in the neuroectoderm (Figures 1I and 1K). At 48 hpf, differentiating neurons form coherent masses of cells covering the entire ventral body side, with the exception of the ventral midline (Figures 1M and 1O). At this stage, *elav* also labels segmental stripes of postmitotic neurons in between the developing appendages (Figures 1Q and 1S). We tentatively identify these as part of the peripheral nervous system (PNS). This is where the sensory "lateral organs" of the trunk, small mechanoreceptive organs with stiff projecting hairs (Purschke and Hausen, 2007), develop. *Elav* expression is excluded from the dorsal-most trunk epithelium.

Combining WMISH with antibody staining against acetylated tubulin, we determined the pattern of early axonal outgrowth in the *Platynereis* trunk neuroectoderm. The pioneer axons of the longitudinal connectives emerge from the early differentiating neurons (Figure 1H; Dorresteijn et al., 1993). At 38 hpf the first commissure appears (Figures 1J–1L), followed by the development of segmental commissures (Figures 1N–1P). Segmental laterally projecting axons appear at 48 hpf (Figure 1R).

We next investigated the tissue architecture of the *Platynereis* neuroepithelium. Mitotically active cells were labeled by BrdU (Figure 2A) and localized to the apical surface of the neuroepithelium by 3D reconstruction of confocal stacks allowing virtual cross-sections (Figures 2B and 2C). In line with this, postmitotic neuronal precursors (expressing *elav*) were excluded from the surface but otherwise spanned the entire neuroepithelium (Figure 2D). In contrast, *synaptotagmin* expression (demarcating differentiating neurons) was restricted to basal cells (Figure 2E), and outgrowing axons ran along the basal surface of the neuroepithelium (arrowheads in Figures 2D and 2E). The *Platynereis* neuroectoderm thus comprises, from apical to basal, a proliferation zone; a progenitor zone containing postmitotic, nondifferentiated neuronal precursors (*elav+, synaptotagmin−*); and a differentiation zone (*elav+, synaptotagmin+*). In line with this, we found that neural specification genes are expressed most apically, in the proliferation and progenitor zones (Figures 2F and 2G); neuronal identity genes more basally in the progenitor and differentiation zones (Figure 2H; and see below); and neuronal differentiation genes most basally in the differentiation zone (Figure 2I; and see below).

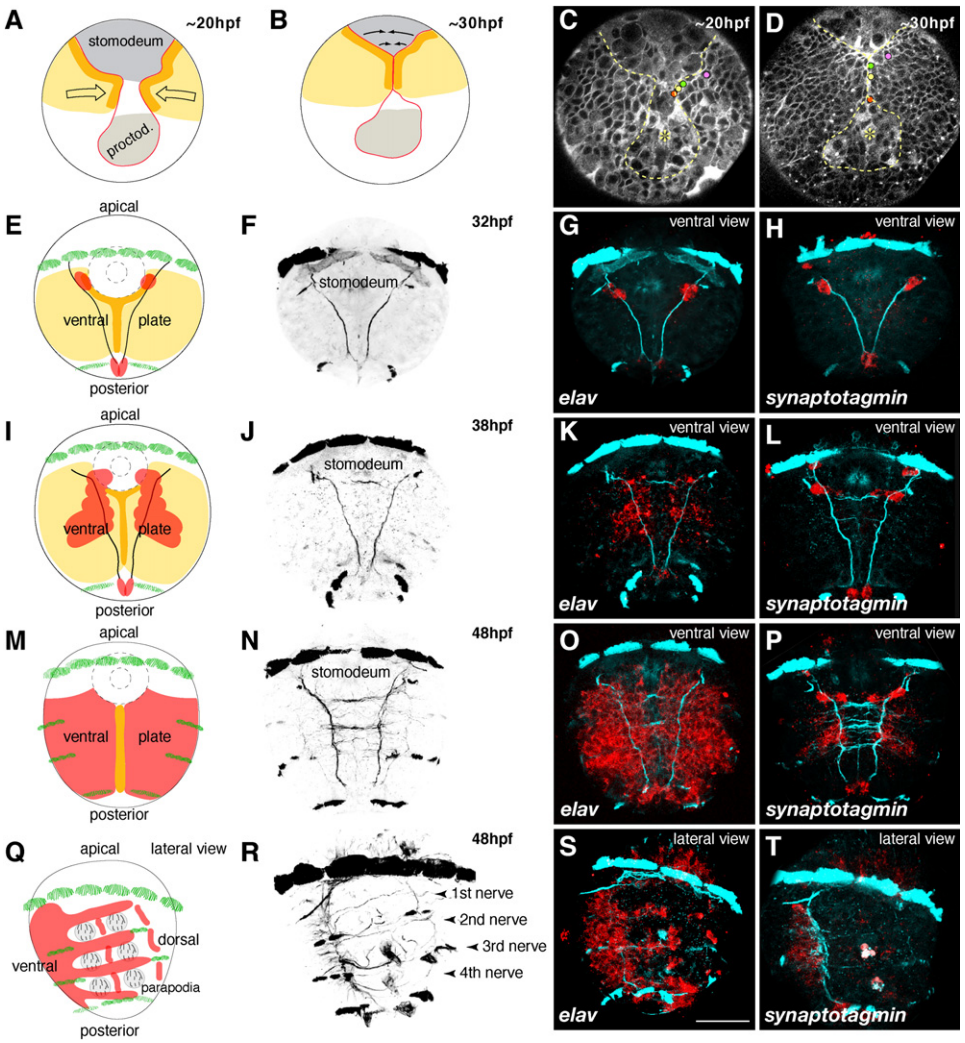

Figure 1. Development of the Trunk Neuroectoderm in *Platynereis*

(A and B) Schematic drawing of neuroectoderm and neural midline formation by zipper-like fusion of the lateral blastopore lips.

(C and D) Two frames from a 580 min timelapse recording of a developing embryo. Cell membranes were labeled with BODIPY564/570-propionic acid. Dashed lines demarcate the blastopore lip. The yellow asterisk indicates a proctodeal cell as a reference point. Colored dots label tracked cells of the prospective neural midline. Neuronal differentiation at 32 hpf (E–H), at 38 hpf (I–L), and at 48 hpf. (ventral view, M–P; lateral view, Q–T).

(E, I, M, and Q) Schematic drawings of larvae with differentiated neurons (red).

(F, J, N, and R) α-acTubulin stainings to label axons and cilia.

WMISH for *elav* (red in G, K, O, S) and *synaptotagmin* (H, L, P, T) counterstained with α-acTubulin (cyan).

(A)–(P) are ventral, and (Q)–(T) are lateral views. In lateral views ventral is to the left. Scale bar is 50 μm.

The *Platynereis* Neuroectoderm Is Subdivided into Vertebrate-Type Longitudinal Progenitor Domains

To investigate the specification of neuronal precursors in the *Platynereis* neuroectoderm, we analyzed the expression of candidate transcription factors at predifferentiation stages (34 hpf). In vertebrates and insects the *nk2.2 (vnd)* gene specifies medial neurons (Briscoe et al., 1999; Wheeler et al., 2005). In *Platynereis*, *nk2.2* expression exhibits a Y-shaped pattern comprising the slender domain of midline cells (Figure 3A) and demarcating the medial edges of the fusing neuroectoderm (compare to Figure 1).

In vertebrates, a broad *pax6*+ progenitor domain laterally abuts the *nk2.2*+ domain from open neural plate stages onward (Ericson et al., 1997). This aspect of early neural patterning is not conserved in the fly (Kammermeier et al., 2001) but is present in *Platynereis* where *Pdu-pax6* is expressed in two longitudinal stripes at predifferentiation stages (Figure 3E). We determined that *nk2.2* and *pax6* expression are also strictly complementary in *Platynereis* (Figures 3B–3D).

The medial part of the *pax6*+ progenitor domain in the vertebrate neural tube overlaps with the lateral part of

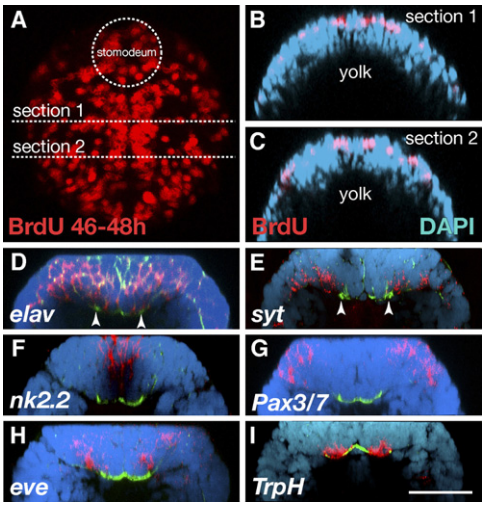

Figure 2. Apicobasal Layering of Proliferation and Neuronal Differentiation Zones

(A) BrdU labeling of a larva between 46–48 hpf.

(B and C) Virtual cross-sections of the larva shown in (A) at two anteroposterior levels and counterstained with DAPI (cyan).

(D–I). Virtual cross-sections of 48 hps WMISH larvae for *elav* (D) and *syt* (E), neural specification (F and G), neuronal identity (H), and neuronal differentiation genes (I) counterstained with α-acTubulin (green) and DAPI (cyan). Arrowheads in (D) and (E) indicate the two connectives. Scale bar is 50 μm.

the *nk6*+ domain (Briscoe et al., 2000). At predifferentiation stages *Pdu-nk6* expression also covers a single broad medial domain (Figure 3I) that overlaps with the medial half of the *pax6* domain (Figures 3J–3L). Thus, the *Platynereis* neuroectoderm is subdivided into a medial *nk2.2*+/*nk6*+ and an intermediate *pax6*+/*nk6*+ neurogenic domain.

Another feature of vertebrate neural patterning not conserved in the fly is the activity of *pax3* and *pax7* in lateral longitudinal progenitor domains (Ericson et al., 1996; Goulding et al., 1993). We found *Platynereis pax3/7* expressed at predifferentiation stages in a lateral longitudinal domain on each side with clear medial boundaries (Figure 3M). In vertebrates, *pax3* and *pax7* largely overlap with *pax6* expression (Pattyn et al., 2003b), and we observed the same for *Pdu-pax3/7* and *Pdu-pax6* (Figures 3F–3H).

Next, in the vertebrate dorsal neural tube the domain of *pax3* and *pax7* activity laterally overlaps with that of the *msx*1 and *msx2* genes (Ramos and Robert, 2005). *Pdu-msx* is similarly expressed in the lateral neuroectoderm (Figure 3S). *Pdu-msx* expression and *Pdu-pax3/7* expression partly overlap as we could determine by costaining WMISH samples with anti-acetylated tubulin antibody and correlating the expression patterns to morphological landmarks such as axons, developing protonephridia and ciliated cells (Figures 3Q–3S). We thus identified a lateral *msx*+/*pax3/7*+ domain similar to that in the dorsal neural tube. In vertebrates, transcription factors of the *dlx* gene family are expressed at the neural plate border and repress neural plate fate (McLarren et al., 2003). We found *Pdu-dlx* expressed in prominent lateral bands overlapping *msx* expression and medially abutting *pax3/7* expression (compare Figures 3S and 3T).

Finally, we also noted differences between the early mediolateral molecular subdivisions of the *Platynereis* and vertebrate neuroectoderm. While in vertebrates the *dbx*+ progenitor domains are located in the gap between the *pax7*+ and the *nk6*+ domains (Briscoe et al., 2000), in *Platynereis pax3/7* expression directly abuts *nk6* expression (Figures 3N–3P). In line with this, we did not find *Pdu-dbx* expressed prior to differentiation stages (see below). In addition, *Pdu-gsx* is not expressed prior to differentiation stages (see below).

Midline, Serotonergic, and Cholinergic Neurons Develop from Corresponding Mediolateral Domains in *Platynereis* and in Vertebrates

We next investigated the mediolateral distribution of selected early differentiating neuron types in 48 hpf larvae (Figure 4A). First, we found that midline cells (compare Figure 1) express *sim* (Figure 4B), a conserved midline-specific transcription factor (Arendt and Nübler-Jung, 1999); *slit* (Figure 4C) encoding a conserved extracellular midline repellent (Brose et al., 1999; Kidd et al., 1999); and *netrin* (Figure 4D) encoding a diffusible chemotropic factor expressed in the midline of various bilaterians (Serafini et al., 1994; Shimeld, 2000). This corroborates evolutionary conservation of midline cells (Arendt and Nübler-Jung, 1999).

Second, we looked at early neural progeny from the medial *nk2.2*+ domain (Figure 4E). We found that the first-appearing bilateral pair of serotonergic neurons in the trunk CNS (Figure 4F) emerges from *nk2.2*+ precursors, as evidenced by double in situ hybridization with the *Platynereis tryptophane hydroxylase (Pdu-TrpH)* gene encoding the rate-limiting enzyme in serotonin biosynthesis (Figure 4G). This is reminiscent of the vertebrate situation where multiple populations of serotonergic neurons differentiate from the *nk2.2*+ domain of the hindbrain and depend on *nkx2.2* in mouse (Briscoe et al., 1999; Pattyn et al., 2003a). They send out ascending projections into the forebrain and descending projections into the spinal cord to modulate spontaneous locomotor activity (Schmidt and Jordan, 2000; Zhang and Grillner, 2000). We analyzed axonal projections of serotonergic neurons in *Platynereis* and found them pioneering the longitudinal tracts (Figure 4I) and segmental nerves (Figures 4J and 4K). The latter project dorsally and coalesce into a continuous dorsal nerve that projects onto the surface of the dorsal longitudinal muscle (Figure 4J). We observed varicosities on the surface of muscle fibers indicative of serotonergic synapses (white arrowheads in Figure 4J). Consistent with direct serotonergic control of muscular activity, a serotonin receptor antagonist, mianserin, inhibited the regular spontaneous contractions of longitudinal muscles (Figure 4L). Apart from the serotonergic neurons, we also found a population of *gsx*+ cells emerging

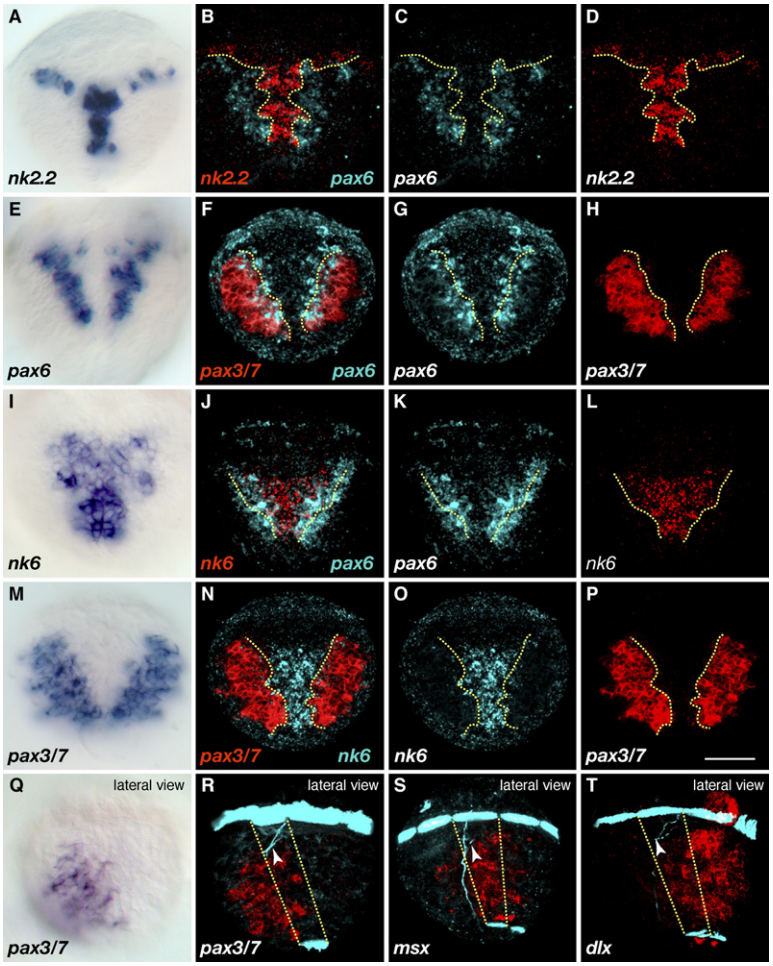

Figure 3. Longitudinal Expression Domains of *pax* and *nk* Genes in the Ventral Neuroectoderm of 34 hpf Larvae

(A) WMISH for *nk2.2*.

(B–D) Double WMISH for *nk2.2* (red) and *pax6* (cyan).

(E) WMISH for *pax6*.

(F–H) Double WMISH for *pax3/7* (red) and *pax6* (cyan).

(I) WMISH for *nk6*.

(J–L) Double WMISH for *nk6* (red) and *pax6* (cyan).

(M) WMISH for *pax3/7*

(N–P) Double WMISH for *pax3/7* (red) and *nk6* (cyan).

WMISH for *pax3/7* (Q and R), *msx* (S), and *dlx* (T).

The thin line demarcates the boundary of the *nk2.2* (B–D), the *pax3/7* (F–H; N–P), and the *nk6* (J–K) domains. (A–P) are ventral, and (Q–T) are lateral views. In lateral views ventral is to the left. Scale bar is 50 μm.

from the *nk2.2*+ domain (Figure 4H). These cells do not find a counterpart in the vertebrate neural tube where *nk2.2* and *gsx* expression do not overlap (see discussion).

Third, we focused on neuron types emerging from the *pax6*+/*nk6*+ progenitor domain. In the vertebrates this domain produces cholinergic somatic motoneurons that depend on *pax6* (Ericson et al., 1997; Osumi et al., 1997). In *Platynereis*, we found that the overlap region of *pax6*+ (Figure 4M) and *nk6*+ (Figure 4N) also gives rise to two bilateral stripes of cholinergic neurons, demarcated by *Choline Acetyltransferase (Pdu-ChAT)* expression (Figure 4O) and *Vesicular Acetylcholine Transporter (Pdu-VAChT)* expression (Figure 4P for coexpression with *pax6*). We further assayed expression of *hb9/mnx*, a conserved somatic motor neuron marker (Arber et al., 1999) and indeed found *hb9*+ cells in the medial *pax6* domain (Figure 4Q), consistent with a somatic cholinergic motoneuron identity (compare Figures 4P and 4Q). In line with this, virtual cross-sections of *pax6-, hb9-,* and *VAChT*-stained larvae at the level of the first commissure indicate the presence of cells coexpressing all three genes (Figures 4R–4T). To investigate cholinergic innervation of the larval musculature we stained for acetylcholinesterase (AChE) activity (Karnovsky and Roots, 1964). AChE, expressed by both cholinergic neurons and their target muscle cells, is known to localize to the synaptic cleft of the neuromuscular junction where it hydrolyzes ACh released by the motoneuron (Rotundo, 2003). We found that the dorsal and the ventral longitudinal muscles were strongly positive for AChE activity (Figure 4U), indicating that they are under cholinergic control. To directly test cholinergic motor control of longitudinal muscles we measured their activity in the presence of a nicotinic ACh receptor antagonist, mecamylamine. Compared to nontreated larvae, exogenous application of mecamylamine decreased the rate of spontaneous longitudinal muscle contractions (Figure 4V). These data show that cholinergic motoneurons directly innervate longitudinal muscles.

Next, we tested for the presence of conserved interneuron types (Figure 5A). In the vertebrate neural tube, numerous interneuron types emerge from the *dbx*+ domain (Moran-Rivard et al., 2001) including the *evx1/2*+ V0 interneurons (Moran-Rivard et al., 2001; Pierani et al., 2001). In *Platynereis*, although an early *dbx*+ progenitor domain

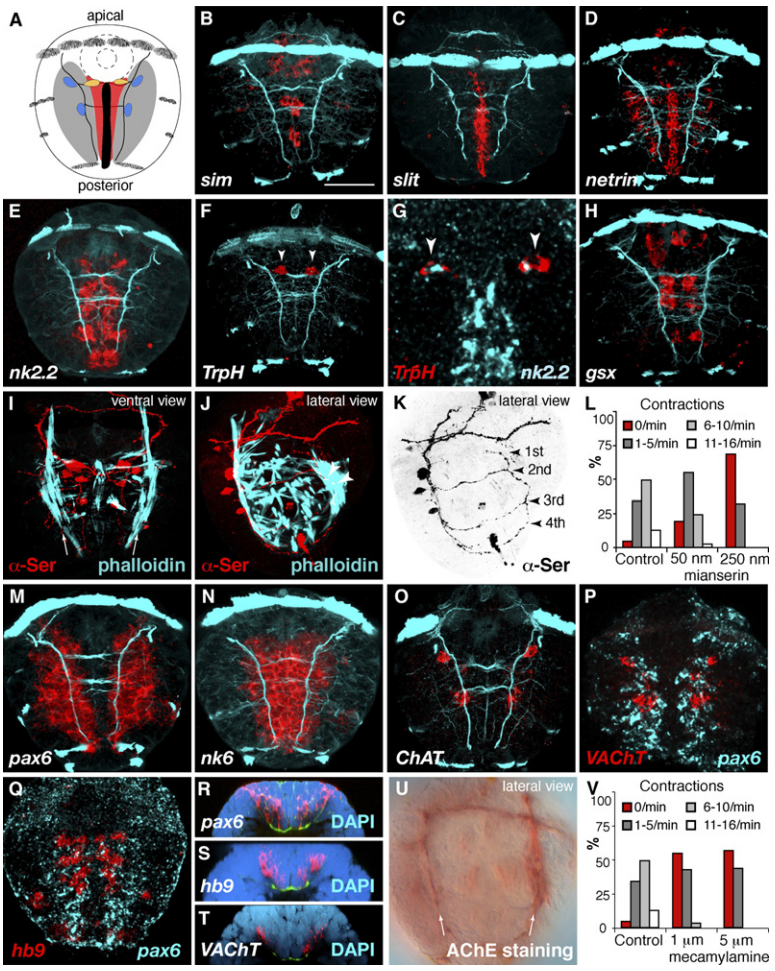

Figure 4. Differentiation of Neuron Types in the Trunk Neuroectoderm in *Platynereis*

(A) Schematic drawing of a 48 hpf larva with the *nk2.2* (red) and *pax6* (gray) domains, early differentiating midline (black), and serotonergic (yellow) and cholinergic cells (blue).

WMISH for *sim* (B), *slit* (C) *netrin* (D), *nk2.2* (E), and *TrpH* (F) counterstained with α-acTubulin (cyan).

(G) Double WMISH for *TrpH* (red) and *nk2.2* (cyan).

(H) WMISH for *gsx*.

(I–K) Serotonergic cell bodies and axons stained with an α-serotonin antibody (red in I and J; black in K) combined with rhodamine-phalloidin stainings (cyan in I and J) to label trunk muscles.

(L) Quantification of longitudinal muscle contractions in 50–54 hpf larvae in the presence of a serotonin-receptor antagonist, mianserin (n > 33 larvae).

WMISH for *pax6* (M), *nk6* (N), and *ChAT* (O).

(P) Double WMISH for *VAChT* (red) and *pax6* (cyan).

(Q) Double WMISH for *hb9* (red) and *pax6* (cyan).

Virtual cross-sections of 48 hps WMISH larvae for *pax6* (R), *hb9* (S), and VAChT (T) counterstained with α-acTubulin (green) and DAPI (cyan).

(U) Lateral view of a larva stained for the activity of AChE. Longitudinal muscles are labeled with arrows.

(V) Quantification of longitudinal muscle contractions in 50–54 hpf larvae in the presence of an ACh-receptor antagonist, mecamylamine (n > 41 larvae). All larvae shown are 48 hpf. (A)–(I) and (M)–(Q) are ventral, and (J), (K), and (U) are lateral views. In lateral views ventral is to the left. Scale bar is 50 μm.

does not exist (see above), we detected restricted populations of *dbx*+ neurons (Figure 5B) at the same mediolateral coordinates as *evx*+ neurons (Figure 5C) and within the *pax6*+/*nk6*+ overlap region (cf. Figures 4M and 4N). Another type of neuron that emerges from the *pax6*+/*nk6*+ domain in the vertebrate neural tube is the *chx10*+ interneuron (Ericson et al., 1997; Vallstedt et al., 2001). We accordingly found *Pdu-chx10/vsx* expressed in the *Platynereis pax6*+/*nk6*+ stripe (Figure 5D; but also more broadly in more lateral regions of the *Platynereis* neuroepithelium). In the vertebrates, *pax2* is required for populations of dorsal interneurons (Burrill et al., 1997). The Platynereis *pax2/5/8* gene is similarly expressed laterally (Figure 5E), where it largely overlaps *pax3/7* (Figure 5F) and *pax6* (compare Figure 4M) as it does in the vertebrates.

By comparing *pax3/7* (Figure 5G) with *elav* (Figure 1S) expression we could determine that the neuroectoderm ends with the lateral edge of the *pax3/7*+ domain, while most of the *dlx*+ ectoderm (Figure 5H) is nonneural. Still, we found *dlx* coexpressed with single cells positive for the sensory marker *atonal (Pdu-ath;* Figures 5I and 5J; Boekhoff-Falk, 2005). Another restricted lateral population of cells emerging from lateral *dlx*+ regions expressed the TRP-family cation channel *trpv* (Figures 5K and 5L; compare to Figure 3T), a sensory receptor in both fly and vertebrates (Boekhoff-Falk, 2005). We thus identified *ath*+ and *trpv*+ sensory cells emerging from the lateral *dlx*+ region as reported for vertebrate and fly.

Bmp Mediates Dose-Dependent Regulation of Mediolateral Specification Genes in the *Platynereis* Neuroectoderm

We next addressed the question of whether mediolateral patterning of the *Platynereis* neuroectoderm involves Dpp/Bmp signaling. Insect Dpp and vertebrate Bmps act in two phases (Bier, 1997; reviewed in Lowe et al., 2006): In the first, they trigger the segregation of neuroectoderm versus epidermal ectoderm. In the second, they contribute to mediolateral neuroectodermal patterning

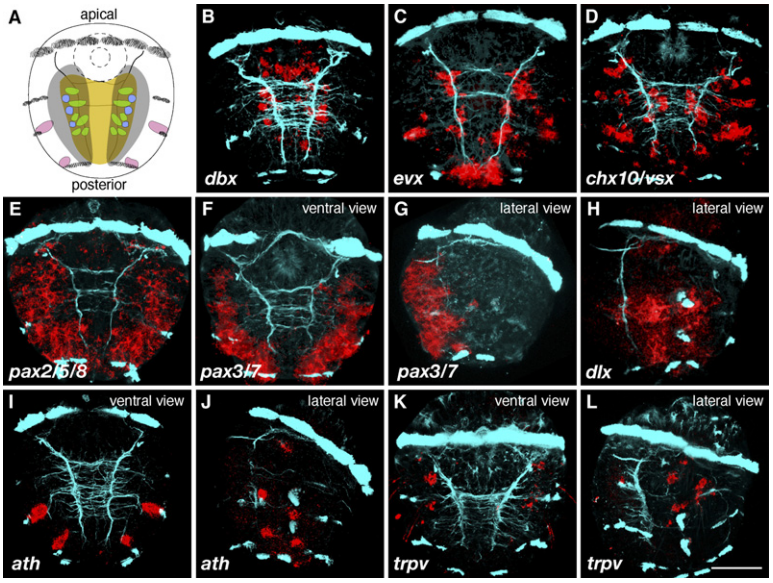

Figure 5. Combinatorial Code of Transcription Factors

(A) Schematic drawing of a 48 hpf larva with the *nk6* (yellow) and *pax6* (gray) domains and the differentiating *evx*+ (green) and *dbx*+ neurons (cyan) as well as the lateral *ath*+ sensory neurons (purple).

WMISH for *dbx* (B), *evx* (C), *chx10/vsx* (D), *pax2/5/8* (E), *pax3/7* (F and G), *dlx* (H), *ath* (I and J), and *trpv* (K and L) counterstained with α-acTubulin (cyan). All larvae shown are 48 hpf. (A)–(F), (I), and (K) are ventral, (G), (H), (J), and (L) are lateral views. In lateral views ventral is to the left. Scale bar is 50 μm.

by differentially down- or upregulating neural specification genes (Mizutani et al., 2006; Rusten et al., 2002). Yet, in enteropneusts a recent study found no evidence for repression of neural genes by Bmp4 (Lowe et al., 2006), calling the common ancestry of the insect and vertebrate Dpp/Bmp regulation of neural genes into question. For *Platynereis,* we determined that the *Pdu-bmp2/4* gene is indeed expressed on the dorsal body side (Figures 6A and 6B). Spatially relating its expression to that of *pax3/7,* we found the ventral CNS neuroectoderm devoid of *bmp2/4* expression (compare Figure 6A to Figure 3R). Yet, we detected a clear overlap of *bmp2/4* with *elav*+ postmitotic peripheral neurons including the *ath*+ cells (compare Figure 6B to Figures 1S and 5J).

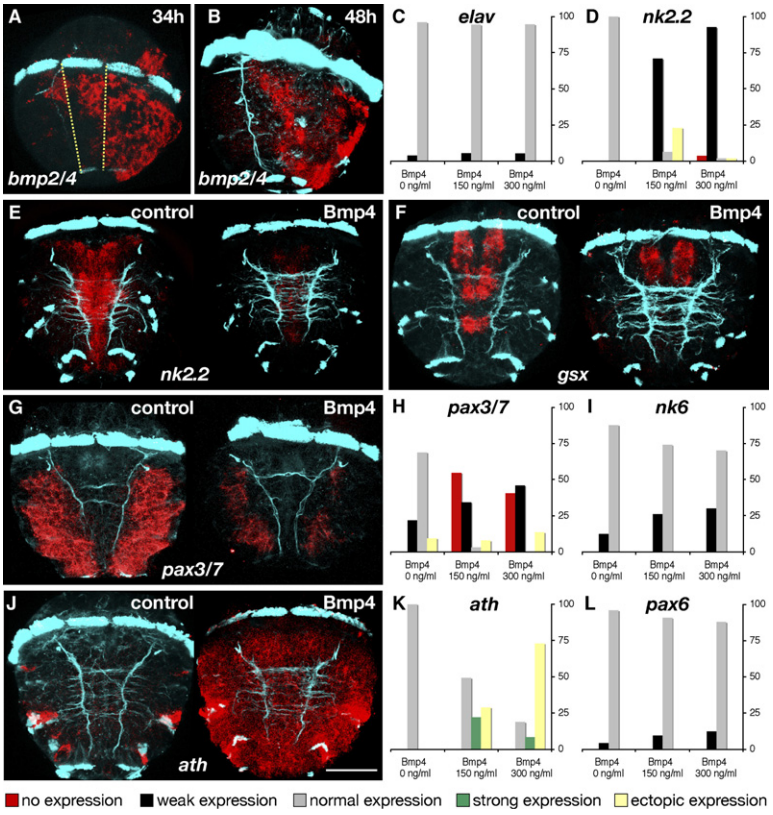

Figure 6. Dose-Dependent Regulation of Mediolateral Patterning Genes by Bmp4

(A) WMISH for *bmp2/4* at 34 hpf and (B) 48 hpf. The larvae are laterally oriented with ventral to the left.

(C and D) Quantification of the effect of Bmp4 on the expression of *elav* (C; n > 100) and *nk2.2* (D; n > 48) by WMISH.

(E–G) WHISM for *nk2.2* (E), *gsx* (F), and *pax3/7* (G) in control and Bmp4-treated embryos counterstained with α-acTubulin (cyan).

(H and I) Quantification of the effect of Bmp4 on the expression of *pax3/7* (H; n > 37) and *nk6* (I; n > 89) by WMISH.

(J) WHISM for *ath* in control and Bmp4-treated embryos counterstained with an anti-acetylated tubulin antibody (cyan).

(K and L) Quantification of the effect of Bmp4 on the expression of *ath* (K; n > 45) and *pax6* (L; n > 142) by WMISH.

The larvae in (E), (F), (G), and (J) are ventrally oriented. Scale bar is 50 μm.

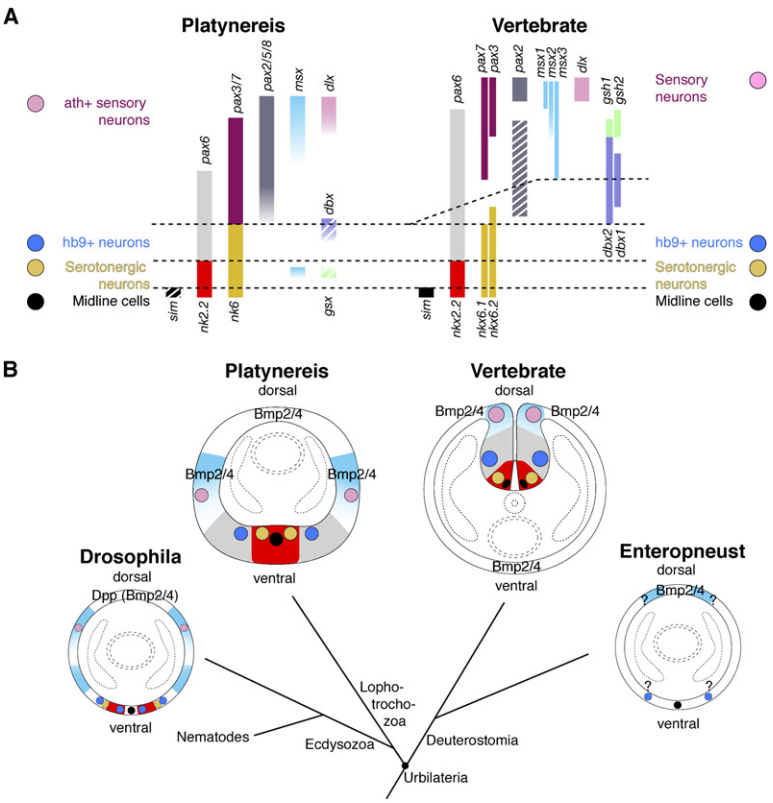

Figure 7. Mediolateral Arrangement of Neurogenic Domains and of Neuron Types in the Annelid and Vertebrate Trunk Nervous Systems

(A) The mediolateral extent of the expression of neural specification genes is represented by vertical bars. Dashed lines separate neurogenic domains with a distinct combination of neural specification genes. Colored bars represent the expression regions of neuronal specification genes at predifferentiation stages. Hatched bars represent genes that are expressed at differentiation stages only.

(B) Comparison of mediolateral patterning in *Platynereis*, vertebrates, *Drosophila* and enteropneust. The schematic drawings represent trunk cross-sections of embryos. The mediolateral extent of expression is shown for *nk2.2* (red), *pax6* (gray), and *msx* (cyan). Midline cells (black), serotonergic neurons (yellow), *hb9+* neurons (blue), and *ath+* lateral sensory neurons (purple) are indicated as circles.

To assay the effect on neural gene expression, we then exposed developing *Platynereis* larvae to increasing concentrations of exogenous Bmp4 protein. First, expression of the neuronal differentiation marker *elav* was left unchanged in Bmp4-treated larvae (Figure 6C). This is in agreement with a similar result in enteropneusts (Lowe et al., 2006) and also rules out a general antineurogenic effect of Dpp/Bmp signaling for *Platynereis*. Second, in *Drosophila*, as in chick, Dpp/Bmp4 downregulates expression of *nk2.2* in a dose-dependent manner (Mizutani et al., 2006), and we found the same for *Platynereis* (Figures 6D and 6E). High concentration of Bmp4 also downregulated the expression of the midline gene *sim* (data not shown) and of *gsx* (Figure 6F) as is also the case in *Drosophila* (Mizutani et al., 2006). Strong, concentration-dependent downregulation by excess Bmp4 was also observed for *Pdu-pax3/7* (Figures 6G and 6H). Third, *nk6* expression was only weakly affected (Figure 6I), and excess Bmp4 did not reduce *pax6* expression at any of the concentrations tested (Figure 6L). Finally, we tested the effect of exogenous Bmp4 on the sensory marker *ath*, which was coexpressed with endogenous *bmp2/4* in the lateral PNS anlage (see above). We found *ath* strongly upregulated in a dose-dependent manner (Figure 6K) so that the normally spot-wise expression expanded into the entire ventral and lateral neuroectoderm (Figure 6J). Together, these findings indicate that in *Platynereis*—as in insects and vertebrates—endogenous Bmp2/4 signaling exerts differential effects on neural patterning genes in CNS and PNS.

DISCUSSION

Common Ancestry of Bilaterian Nervous System Centralization

Given the obvious paucity of information from the fossil record, the main strategy to elucidate CNS evolution is to compare nervous system development in extant forms. Our comparative study of mediolateral neural patterning and neuron-type distribution in the developing trunk CNS of the annelid *Platynereis* revealed an unexpected degree of similarity to the mediolateral architecture of the developing vertebrate neural tube (Figure 7).

First, the *Platynereis* and vertebrate neuroepithelium are similarly subdivided (from medial to lateral) into a *sim+* midline and four longitudinal CNS progenitor domains (*nk2.2+/nk6+*, *pax6+/nk6+*, *pax6+/pax3/7+*, and *msx+/pax3/7+*), laterally bounded by an *msx+, dlx+* territory (Figure 7A). This strongly indicates a common evolutionary origin from an equally complex ancestral pattern. It is highly unlikely that precisely *this* mediolateral order and overlap in expression of orthologous genes in the CNS neuroectoderm should evolve twice independently. One can also discount the possibility that these genes are necessarily linked and thus co-opted as a package because they also act independently of each other in other

developmental contexts (*nk2.2* in endoderm development; *pax6* in eye development, *pax3/7* in segmentation, and *msx* in muscle development). Following similar reasoning, the complex conserved topography of gene expression along the anteroposterior axis in the enteropneust and vertebrate head is considered homologous (Davidson, 2006; Lowe et al., 2003).

Second, we found evidence for conserved neuron types emerging from corresponding domains in *Platynereis* and in vertebrates. Serotonergic neurons involved in locomotor control form from the medial *nk2.2+/nk6+* domain. A conserved population of *hb9+* cholinergic somatic motoneurons emerges from the adjacent *pax6+/nk6+* domain. Neurons expressing interneuron markers are found at the same level and more laterally, and single cells positive for sensory marker genes populate the lateral *dlx+* domain. Notably, our characterization of neuron types in the developing *Platynereis* nervous system is yet incomplete so that the full extent of conservation in neuron type distribution remains to be determined.

Third, Bmp signaling is similarly involved in the dose-dependent control of the neural genes. Our finding that exogenous Bmp4 protein differentially regulates neural patterning genes in *Platynereis* nervous system development corroborates recent evidence that Bmps play an ancestral role in the mediolateral patterning of the bilaterian CNS neuroectoderm (Mizutani et al., 2006). Also, the strong upregulation of *Pdu-atonal* in the larval ectoderm goes in concert with *Drosophila* data that indicate that Dpp signaling positively regulates *atonal* expression in the lateral PNS anlage (Rusten et al., 2002), and it supports the view that Bmp signaling also plays a conserved role in the specification of peripheral sensory neurons (Rusten et al., 2002). Conservation of the molecular mediolateral CNS architecture concomitant with its sensitivity to Bmp signaling indicates that the developmental link between Bmp signaling and nervous system centralization predates Bilateria.

Taken together, our data make a very strong case that the complex molecular mediolateral architecture of the developing trunk CNS, as shared between *Platynereis* and vertebrates, was already present in their last common ancestor, Urbilateria (Figure 7B). The concept of bilaterian nervous system centralization implies that neuron types concentrate on one side of the trunk, as is the case in vertebrates and many invertebrates including *Platynereis* (Figure 1S), where they segregate and become spatially organized (as opposed to a diffuse nerve net). Our data reveal that a large part of the spatial organization of the annelid and vertebrate CNS was already present in their last common ancestor, which implies that Urbilateria had already possessed a CNS.

Modification or Loss of the Complex Mediolateral Architecture in *Drosophila*, Nematode, and Enteropneust

Evolutionary conservation of the molecular mediolateral architecture as shared between *Platynereis* and vertebrates would imply that it was initially present also in the evolutionary lines leading to *Drosophila*, the nematode *Caenorhabditis*, and the enteropneust *Saccoglossus* (Figure 7B). Yet it is clear from the available data that these animals are missing or have modified at least part of this pattern (see Introduction; Figure 7B), although the extent of conservation may actually be larger than is currently apparent. For example, we costained for *nk2.2/vnd* and *pax6* expression in the fly and found a complementary pattern at germ-band-extended stage (Figure S1; Figure 7B), reminiscent of the *Platynereis* and vertebrate situation. Strikingly, however, there is no trace so far of the conserved mediolateral architecture in the nematode *Caenorhabditis* (Okkema et al., 1997) and hardly any in the enteropneust *Saccoglossus* (Lowe et al., 2006). How did this come about? Fly and nematode exhibit very fast development, making it plausible that they have (partially) omitted the transitory formation of longitudinal progenitor domains to speed up neurodevelopment. For the enteropneust, however, the situation is less clear. Why is the pattern absent in an animal that otherwise shows strong evolutionary conservation (for example, the anteroposterior head-patterning genes; Gerhart et al., 2005; Lowe et al., 2003)? One possible explanation is that the enteropneust trunk has lost part of its neuroarchitecture due to an evolutionary change in locomotion. While annelids and vertebrates propel themselves through trunk musculature (and associated trunk CNS), the enteropneust body is mainly drawn forward by means of the contraction of the longitudinal muscles in their anterior proboscis and collar (Dawydoff, 1948; Knight-Jones, 1952). Possibly, enteropneusts have partially reduced their locomotor trunk musculature concomitant with motor parts of the CNS (while the peripheral sensory neurons prevailed in "diffuse" arrangement). In line with this, expression of the conserved somatic motoneuron marker *hb9/mnx* is mostly absent from the *Saccoglossus* trunk ectoderm except for few patches (Lowe et al., 2006). A more detailed understanding of enteropneust nervous system organization, neuron type distribution, and locomotion will help with resolving this issue.

Intercalation and Expansion of *dbx+, gsh+* Interneuron Domains in Vertebrate CNS Evolution

An overall conservation of mediolateral CNS neuroarchitecture as proposed here does not imply that everything is similar. It is clear that the lines of evolution leading to annelids and vertebrates diverged for more than 600 million years, and numerous smaller or larger modifications of the ancestral pattern must have accumulated in both lines. The common-ground pattern as elucidated here helps in identifying these changes. For example, annelid and vertebrate differ in the deployment of *gsx* and *dbx* orthologs (Figure 7). While mouse *gsh* and *dbx* genes act early to specify interneuron progenitor domains in the dorsal neural tube, we found the *Platynereis gsx* and *dbx* genes expressed at differentiation stages only. Adding to this, *Pdu-gsx* is expressed at a different mediolateral position

in the *nk2.2*+ domain, and *Pdu-dbx* expression is much more restricted than that of its vertebrate counterparts (though the overall mediolateral coordinates correspond). We hypothesize that these differences relate to the emergence of new interneuron domains (*gsx*+*; dbx*+) inside of the ancestral *pax6*+/*pax3/7*+ domain in the dorsal vertebrate neural tube (Figure 7). For this, it is conceivable that genes were recruited that had been active already in the differentiation of the diversifying interneuron populations. It is worth mentioning that the role of *gsx* in neuronal development also varies among vertebrates.

DV Axis Inversion and Dohrn's Annelid Theory

Homology of the vertebrate and *Platynereis* mediolateral molecular architecture is inevitably linked to the notion of dorsoventral axis inversion during early chordate evolution. In his 1875 essay on the origin of vertebrates Anton Dohrn discusses the resemblances between vertebrates and annelids and states that "what stands most in the way of such a comparison has been the viewpoint that the nervous system of [annelids] is located in the venter, but that of vertebrates in the dorsum. Hence the one is called the ventral nerve cord, the other the dorsal nerve cord. Had we not possessed the terms dorsal and ventral, then the comparison would have been much easier." How did the relocation of the trunk CNS from ventral to dorsal come about? Anton Dohrn proposed that vertebrate ancestors inverted their entire body dorsoventrally so that the former belly became the new back. This would not necessarily involve a sudden major shift in the lifestyle of an ancestor, as argued by critics of DV axis inversion. One can also imagine that an inversion involved transitional forms, with hemisessile or burrowing lifestyle and changing orientation toward the substrate. These animals had gill slits and lived as filter feeders. Only when early vertebrates left the substrate and acquired a free-swimming lifestyle would their new belly-up orientation have been fixed such that their CNS was then dorsal. Dohrn believed that the foremost gill slits then formed a new mouth on the new ventral body side (Dohrn, 1875). More than 130 years later, our molecular data on annelid neurodevelopment corroborate the key aspect of Dohrn's annelid theory, which is the homology of the annelid and vertebrate trunk CNS.

EXPERIMENTAL PROCEDURES

Whole-Mount In Situ Hybridization and Immunohistochemistry

Platynereis embryos were obtained from an established breeding culture, following Dorresteijn et al. (1993), and were raised at 18°C. Larvae were fixed in 4% PFA in PBS + 0.1% Tween-20, for 2 hr at room temperature and were stored in 100% MeOH at −20°C.

WMISH, double fluorescent WMISH, and fluorescent/NBT-BCIP WMISH were done as described (Tessmar-Raible et al., 2005). Embryos were counterstained with an anti-acetylated tubulin antibody (Sigma T6793) at 1:500. The primary antibody was added together with anti-DIG antibody. After NBT/BCIP staining, embryos were incubated with fluorescent secondary antibodies (Jackson ImmunoResearch) at 1:250 dilution.

For rhodamine phalloidin and anti-serotonin antibody stainings, embryos were fixed for 1 hr and washed 2× in PBS + 0.1% Tween-20, then incubated with a rabbit anti-serotonin antibody (DIASORIN, #13002307) as 1:500. Anti-rabbit Cy5 secondary antibody (Jackson ImmunoResearch) was used as 1:250, and rhodamine-phalloidin (Molecular Probes) was used as 1:500.

Acetylcholinesterase-activity stainings were done by a method adapted from Karnovsky and Roots (1964). Embryos were fixed for 2 min with ice-cold EtOH and stained for 3 hr at 37°C in freshly prepared staining solution (5 mg acetylthiocholine iodide, 6.5 ml 0.1 M sodium maleate pH 6, 0.5 ml 0.1 M sodium citrate, 1 ml 30 mM copper sulfate, 1 ml water, and 1 ml 5 mM potassium ferricyanide). Staining was stopped in 50% EtOH. Embryos were dehydrated through a graded ethanol series and mounted in 87% glycerol.

Isolation of *Platynereis* Genes

Using degenerate primers, we cloned fragments of *Platynereis hb9, nk6, dbx, ChAT, msx, bmp2/4,* and *sim* (see Supplemental Data for primer sequences). As templates, we used a 48 hpf larval cDNA library in pCMV-Sport6 as well as 24 hpf and 48 hpf larval SMART cDNA prepared with the SmartRace kit (BD Bioscience). Other genes were published earlier (*pax6*, *ath*, Arendt et al., 2002; *evx*, de Rosa et al., 2005; *dpp, msx,* and *pax2/5/8*, Raible et al., 2005) or were obtained as ESTs from a 48 hpf library. Orthology of novel genes was checked by molecular phylogeny (see Supplemental Data).

Microscopy

Bright-field images were taken on a Zeiss Axiophot microscope using DIC optics. Confocal images were taken either with a Leica TCS SP2 or a Leica TCS SPE confocal microscope with a 40× oil-immersion objective.

For whole-mount reflection CLSM (Jékely and Arendt, 2007) a 633 nm gas laser or a 635 nm diode laser was used, and the detection window was set to 630–640 nm. It was combined either with fluorescent antibody staining or fluorescent tyramide WMISH and confocal detection of fluorescence using appropriate laser lines. For each embryo, 20–30 1.5 to 2.5 μm thick sections were taken and processed using ImageJ.

Labeling of Cellular Outlines and Timelapse Recordings

Embryos were incubated for 15 min in seawater with 5 μM BODIPY564/570-propionic acid (Molecular Probes) and rinsed twice with 1:1 seawater and 7.5% $MgCl_2$ to paralyze muscles. Recording was performed with a Perkin Elmer Ultraview RS System from approximately 20 to 30 hpf. Embryos were mounted between a slide and a cover slip, separated by two layers of adhesive tape, and sealed with mineral oil (Sigma). Development was faster because embryos were at 25°C, rather than 18°C, during recording. Image analysis was done using NIH Image 1.63 and ImageJ. Images have been enhanced for contrast and adjusted for brightness to correct for bleaching.

Inhibitor Assays and Bmp4 Incubation

50–54 hpf embryos were mounted between a slide and a cover slip separated by three layers of adhesive tape. Mecamylamine and mianserin (Sigma) were added to the seawater before measurements. Muscle contractions were recorded for 2 min for each larva by video microscopy at 10 fps on a Zeiss Axiophot microscope.

For the Bmp4 experiments 24 hpf larvae were incubated in seawater in the presence of different concentrations of recombinant zebrafish Bmp4 (R&D Systems, Cat. No. 1128-BM). After 24 hr incubation, 48 hpf larvae were fixed for WMISH.

Supplemental Data

Supplemental Data include Experimental Procedures, two figures, and one movie and can be found with this article online at http://www.cell.com/cgi/content/full/129/2/277/DC1/.

ACKNOWLEDGMENTS

The authors wish to thank K. Tessmar-Raible for contributing to the starting of the project and all members of the Arendt lab for discussion and support. We are grateful to anonymous referees for helpful comments. B. Mittman provided an initial fragment of *Pdu-msx*. This work was supported by grants from the Marine Genomics Europe Network of Excellence (NoE-MGE [D.A.], GOCE-04-505403 [D.A. and F.R.]) and fellowships of the Marie Curie RTN ZOONET (MRTN-CT-2004-005624 [D.A.]). G.J. was supported by a FEBS Long-Term Fellowship, A.D. by a Louis Jeantet Foundation fellowship, and P.R.H.S. by a fellowship from the Luxembourg ministry of Culture, Higher Education, and Research.

Received: August 4, 2006
Revised: December 22, 2006
Accepted: February 13, 2007
Published: April 19, 2007

REFERENCES

Anderson, D.T. (1966). The comparitive embryology of the Polychaeta. Acta Zool. *47*, 1–42.

Arber, S., Han, B., Mendelsohn, M., Smith, M., Jessell, T.M., and Sockanathan, S. (1999). Requirement for the homeobox gene Hb9 in the consolidation of motor neuron identity. Neuron *23*, 659–674.

Arendt, D., and Nübler-Jung, K. (1994). Inversion of dorsoventral axis? Nature *371*, 26.

Arendt, D., and Nübler-Jung, K. (1999). Comparison of early nerve cord development in insects and vertebrates. Development *126*, 2309–2325.

Arendt, D., Tessmar, K., de Campos-Baptista, M.I., Dorresteijn, A., and Wittbrodt, J. (2002). Development of pigment-cup eyes in the polychaete Platynereis dumerilii and evolutionary conservation of larval eyes in Bilateria. Development *129*, 1143–1154.

Bier, E. (1997). Anti-neural-inhibition: a conserved mechanism for neural induction. Cell *89*, 681–684.

Boekhoff-Falk, G. (2005). Hearing in Drosophila: development of Johnston's organ and emerging parallels to vertebrate ear development. Dev. Dyn. *232*, 550–558.

Bossing, T., Udolph, G., Doe, C.Q., and Technau, G.M. (1996). The embryonic central nervous system lineages of Drosophila melanogaster. I. Neuroblast lineages derived from the ventral half of the neuroectoderm. Dev. Biol. *179*, 41–64.

Briscoe, J., Sussel, L., Serup, P., Hartigan-O'Connor, D., Jessell, T.M., Rubenstein, J.L., and Ericson, J. (1999). Homeobox gene Nkx2.2 and specification of neuronal identity by graded Sonic hedgehog signalling. Nature *398*, 622–627.

Briscoe, J., Pierani, A., Jessell, T.M., and Ericson, J. (2000). A homeodomain protein code specifies progenitor cell identity and neuronal fate in the ventral neural tube. Cell *101*, 435–445.

Brose, K., Bland, K.S., Wang, K.H., Arnott, D., Henzel, W., Goodman, C.S., Tessier-Lavigne, M., and Kidd, T. (1999). Slit proteins bind Robo receptors and have an evolutionarily conserved role in repulsive axon guidance. Cell *96*, 795–806.

Burrill, J.D., Moran, L., Goulding, M.D., and Saueressig, H. (1997). PAX2 is expressed in multiple spinal cord interneurons, including a population of EN1+ interneurons that require PAX6 for their development. Development *124*, 4493–4503.

Cheesman, S.E., Layden, M.J., Von Ohlen, T., Doe, C.Q., and Eisen, J.S. (2004). Zebrafish and fly Nkx6 proteins have similar CNS expression patterns and regulate motoneuron formation. Development *131*, 5221–5232.

Davidson, E.H. (2006). The Regulatory Genome (Burlington, MA: Academic Press).

Dawydoff, G. (1948). Classe des Entéropneustes. In Traité de Zoologie, P.P. Grassé, ed. (Paris: Masson), pp. 369–489.

De Robertis, E.M., and Sasai, Y. (1996). A common groundplan for dorsoventral patterning in Bilateria. Nature *380*, 37–40.

de Rosa, R., Prud'homme, B., and Balavoine, G. (2005). Caudal and even-skipped in the annelid Platynereis dumerilii and the ancestry of posterior growth. Evol. Dev. *7*, 574–587.

Dohrn, A. (1875). Der Ursprung der Wirbelthiere und das princip des Functionswechsels (Leipzig: Wilhelm Engelmann).

Dorresteijn, A.W.C., O'Grady, B., Fischer, A., Porchet-Henere, E., and Boilly-Marer, Y. (1993). Molecular specification of cell lines in the embryo of *Platynereis* (Annelida). Rouxs Arch. Dev. Biol. *202*, 264–273.

Ericson, J., Morton, S., Kawakami, A., Roelink, H., and Jessel, T.M. (1996). Two critical periods of Sonic Hedgehog signaling required for the specification of motor neuron identity. Cell *87*, 661–673.

Ericson, J., Rashbass, P., Schedl, A., Brenner-Morton, S., Kawakami, A., van Heyningen, V., Jessell, T.M., and Briscoe, J. (1997). Pax6 controls progenitor cell identity and neuronal fate in response to graded Shh signaling. Cell *90*, 169–180.

Gerhart, J., Lowe, C., and Kirschner, M. (2005). Hemichordates and the origin of chordates. Curr. Opin. Genet. Dev. *15*, 461–467.

Goulding, M.D., Lumsden, A., and Gruss, P. (1993). Signals from the notochord and floor plate regulate the region-specific expression of two Pax genes in the developing spinal cord. Development *117*, 1001–1016.

Halanych, K.M., Bacheller, J.D., Aguinaldo, A.M., Liva, S.M., Hillis, D.M., and Lake, J.A. (1995). Evidence from 18S ribosomal DNA that the lophophorates are protostome animals. Science *267*, 1641–1643.

Hatschek, B. (1878). Studien über Entwicklungsgeschichte der Anneliden. Arb. Zool. Inst. Wien *11*, 1–88.

Holland, N.D. (2003). Early central nervous system evolution: an era of skin brains? Nat. Rev. Neurosci. *4*, 1–11.

Jékely, G., and Arendt, D. (2007). Cellular resolution expression profiling using confocal detection of NBT/BCIP precipitate by reflection microscopy. BioTechniques, in press. Published online May 1, 2007.

Jessell, T.M. (2000). Neuronal specification in the spinal cord: inductive signals and transcriptional codes. Nat. Rev. Genet. *1*, 20–29.

Kammermeier, L., Leemans, R., Hirth, F., Flister, S., Wenger, U., Walldorf, U., Gehring, W.J., and Reichert, H. (2001). Differential expression and function of the Drosophila Pax6 genes eyeless and twin of eyeless in embryonic central nervous system development. Mech. Dev. *103*, 71–78.

Karnovsky, M.J., and Roots, L. (1964). A "direct-coloring" thiocholine method for cholinesterases. J. Histochem. Cytochem. *12*, 219–221.

Kidd, T., Bland, K.S., and Goodman, C.S. (1999). Slit is the midline repellent for the robo receptor in Drosophila. Cell *96*, 785–794.

Knight-Jones, E.W. (1952). On the nervous system of Saccoglossus cambrensis (Enteropneusta). Philos. Trans. R. Soc. Lond. B Biol. Sci. *236*, 315–354.

Kriks, S., Lanuza, G.M., Mizuguchi, R., Nakafuku, M., and Goulding, M. (2005). Gsh2 is required for the repression of Ngn1 and specification of dorsal interneuron fate in the spinal cord. Development *132*, 2991–3002.

Lowe, C.J., Wu, M., Salic, A., Evans, L., Lander, E., Stange-Thomann, N., Gruber, C.E., Gerhart, J., and Kirschner, M. (2003). Anteroposterior patterning in hemichordates and the origins of the chordate nervous system. Cell *113*, 853–865.

Lowe, C.J., Terasaki, M., Wu, M., Freeman, R.M., Jr., Runft, L., Kwan, K., Haigo, S., Aronowicz, J., Lander, E., Gruber, C., et al. (2006).

Dorsoventral patterning in hemichordates: insights into early chordate evolution. PLoS Biol. *4*, e291. 10.1371/journal.pbio.0040291.

McLarren, K.W., Litsiou, A., and Streit, A. (2003). DLX5 positions the neural crest and preplacode region at the border of the neural plate. Dev. Biol. *259*, 34–47.

Mizutani, C.M., Meyer, N., Roelink, H., and Bier, E. (2006). Threshold-dependent BMP-mediated repression: a model for a conserved mechanism that patterns the neuroectoderm. PLoS Biol. *4*, e313. 10.1371/journal.pbio.0040313.

Moran-Rivard, L., Kagawa, T., Saueressig, H., Gross, M.K., Burrill, J., and Goulding, M. (2001). Evx1 is a postmitotic determinant of v0 interneuron identity in the spinal cord. Neuron *29*, 385–399.

Okkema, P.G., Ha, E., Haun, C., Chen, W., and Fire, A. (1997). The Caenorhabditis elegans NK-2 homeobox gene ceh-22 activates pharyngeal muscle gene expression in combination with pha-1 and is required for normal pharyngeal development. Development *124*, 3965–3973.

Osumi, N., Hirota, A., Ohuchi, H., Nakafuku, M., Iimura, T., Kuratani, S., Fujiwara, M., Noji, S., and Eto, K. (1997). Pax-6 is involved in the specification of hindbrain motor neuron subtype. Development *124*, 2961–2972.

Pattyn, A., Vallstedt, A., Dias, J.M., Samad, O.A., Krumlauf, R., Rijli, F.M., Brunet, J.F., and Ericson, J. (2003a). Coordinated temporal and spatial control of motor neuron and serotonergic neuron generation from a common pool of CNS progenitors. Genes Dev. *17*, 729–737.

Pattyn, A., Vallstedt, A., Dias, J.M., Sander, M., and Ericson, J. (2003b). Complementary roles for Nkx6 and Nkx2 class proteins in the establishment of motoneuron identity in the hindbrain. Development *130*, 4149–4159.

Pierani, A., Moran-Rivard, L., Sunshine, M.J., Littman, D.R., Goulding, M., and Jessell, T.M. (2001). Control of interneuron fate in the developing spinal cord by the progenitor homeodomain protein Dbx1. Neuron *29*, 367–384.

Poskanzer, K.E., Marek, K.W., Sweeney, S.T., and Davis, G.W. (2003). Synaptotagmin I is necessary for compensatory synaptic vesicle endocytosis in vivo. Nature *426*, 559–563.

Purschke, G., and Hausen, G.P. (2007). Lateral organs in sedentary polychaetes (Annelida) - Ultrastructure and phylogenetic significance of an insufficiently known sensory organ. Acta Zool *88*, 23–39.

Raible, F., Tessmar-Raible, K., Oseogawa, K., Wincker, P., Jubin, C., Balavoine, B., Ferrier, D.E., Benes, V., de Jong, P., Weissenbach, J., et al. (2005). Vertebrate-type intron-rich genes in the marine annelid *Platynereis dumerilii*. Science *310*, 1325–1326.

Ramos, C., and Robert, B. (2005). msh/Msx gene family in neural development. Trends Genet. *21*, 624–632.

Rotundo, R.L. (2003). Expression and localization of acetylcholinesterase at the neuromuscular junction. J. Neurocytol. *32*, 743–766.

Rusten, T.E., Cantera, R., Kafatos, F.C., and Barrio, R. (2002). The role of TGF beta signaling in the formation of the dorsal nervous system is conserved between Drosophila and chordates. Development *129*, 3575–3584.

Schmidt, B.J., and Jordan, L.M. (2000). The role of serotonin in reflex modulation and locomotor rhythm production in the mammalian spinal cord. Brain Res. Bull. *53*, 689–710.

Schmidt, H., Rickert, C., Bossing, T., Vef, O., Urban, J., Technau, G.M., Udolph, G., and Doe, C.Q. (1997). The embryonic central nervous system lineages of Drosophila melanogaster. II. Neuroblast lineages derived from the dorsal part of the neuroectoderm. Dev. Biol. *189*, 186–204.

Serafini, T., Kennedy, T.E., Galko, M.J., Mirzayan, C., Jessell, T.M., and Tessier-Lavigne, M. (1994). The netrins define a family of axon outgrowth-promoting proteins homologous to C. elegans UNC-6. Cell *78*, 409–424.

Shimeld, S. (2000). An amphioxus netrin gene is expressed in midline structures during embryonic and larval development. Dev. Genes Evol. *210*, 337–344.

Soller, M., and White, K. (2004). Elav. Curr. Biol. *14*, R53.

Tessmar-Raible, K., Steinmetz, P.R.H., Snyman, H., Hassel, M., and Arendt, D. (2005). Fluorescent two color whole-mount in situ hybridization in Platynereis dumerilii (Polychaeta, Annelida), an emerging marine molecular model for evolution and development. Biotechniques *39*, 460–464.

Vallstedt, A., Muhr, J., Pattyn, A., Pierani, A., Mendelsohn, M., Sander, M., Jessell, T.M., and Ericson, J. (2001). Different levels of repressor activity assign redundant and specific roles to Nkx6 genes in motor neuron and interneuron specification. Neuron *31*, 743–755.

Weiss, J.B., Von Ohlen, T., Mellerick, D.M., Dressler, G., Doe, C.Q., and Scott, M.P. (1998). Dorsoventral patterning in the Drosophila central nervous system: the intermediate neuroblasts defective homeobox gene specifies intermediate column identity. Genes Dev. *12*, 3591–3602.

Wheeler, S.R., Carrico, M.L., Wilson, B.A., and Skeath, J.B. (2005). The Tribolium columnar genes reveal conservation and plasticity in neural precursor patterning along the embryonic dorsal-ventral axis. Dev. Biol. *279*, 491–500.

Wilson, E.B. (1892). The cell-lineage of *Nereis*. A contribution to the cytogeny of the annelid body. J. Morphol. *6*, 361–480.

Zhang, W., and Grillner, S. (2000). The spinal 5-HT system contributes to the generation of fictive locomotion in lamprey. Brain Res. *879*, 188–192.